Vol. 600: 41–53, 2018
https://doi.org/10.3354/meps12643

MARINE ECOLOGY PROGRESS SERIES
Mar Ecol Prog Ser

Published July 30

Mixing regime-dependent causality between phytoplankton and bacteria in the subtropical North Atlantic Ocean ecosystem

Hyewon Kim[1,3,*], Dong Eun Lee[2], Hugh W. Ducklow[1]

[1]Division of Biology and Paleo Environment, Lamont-Doherty Earth Observatory, Columbia University, Palisades, NY 10964, USA
[2]Division of Ocean and Climate Physics, Lamont-Doherty Earth Observatory, Columbia University, Palisades, NY 10964, USA
[3]*Present address:* Department of Environmental Sciences, University of Virginia, Charlottesville, VA 22904, USA

ABSTRACT: Ever since marine heterotrophic bacteria were understood to mediate carbon fluxes to upper trophic levels via the microbial loop, quantifying the coupling between bacteria and phytoplankton has been one of the main priorities for marine microbiologists. The complex nature of phytoplankton–bacterial interactions may lead to nonlinear and regime-dependent coupling, for which conventional statistical approaches such as cross-correlation provide an incomplete picture of the dynamics. Here, we employed a nonlinear method for detecting causality, called convergent cross mapping (CCM), to examine a causal linkage between phytoplankton (primary production) and bacteria (bacterial production) at the Bermuda Atlantic Time-series Study (BATS) site. First, we verified the robustness of our CCM models with synthetic time series output from the Fasham-Ducklow-McKelvie ecosystem model. Initially, we hypothesized a strong bi-directional causal link between phytoplankton and bacteria due to the importance of the microbial loop at BATS. However, the results from our CCM models highlight that phytoplankton–bacterial causal coupling depends on seasonally distinct mixing regimes. While there was no evidence for bi-directional causality between phytoplankton and bacteria during the mixing period, moderate unidirectional causality of bacteria on phytoplankton was detected during the stratification period. Our study reveals causal associations between the 2 major microbial loop processes, for which better quantification is needed to improve our understanding of carbon cycling and export via microbial food webs.

KEY WORDS: Convergent cross mapping · CCM · Bermuda Atlantic Time-series Study · BATS · Primary production · Bacterial production · Sargasso Sea

INTRODUCTION

In ocean food webs, microorganisms mediate a large fraction of the energy flow and dictate major fluxes and cycling of biologically important elements, such as C, N, and P (Pomeroy 1974). Microbial ecologists have gained a mechanistic understanding of biogeochemical roles of microbial loop components by focusing on interactions between marine aerobic heterotrophic bacteria (hereafter, 'bacteria') and phytoplankton (Azam et al. 1983, Cole et al. 1988). Phytoplankton influence bacteria by providing organic carbon sources (i.e. dissolved organic carbon, DOC) for bacterial biomass synthesis, whereas bacteria influence phytoplankton by remineralizing organic material to essential inorganic nutrients for phytoplankton growth (i.e. regenerated production) and by providing key compounds such as soluble B vitamins and trace metal ligands (Taylor & Sullivan 2008, Sañudo-Wilhelmy et al. 2014). Theoretically, these

*Corresponding author: hk8m@virginia.edu

interactions provide a mathematical basis for dynamic coupling between these 2 microbial groups. The degree of bacterial–phytoplankton coupling and interactions in microbial food web dynamics might ultimately impact the efficiency of the biological pump and carbon export and fluxes (Legendre & Le Fèvre 1991, Siegel et al. 2016). Bacterial–phytoplankton coupling is particularly important in oligotrophic oceanic environments where microbial food webs are dominant (Steinberg et al. 2001). However, quantifying bacterial–phytoplankton coupling itself may not be a simple task. Though numerous ecosystem models provide underlying equations to dictate bi-directional interactions between phytoplankton and bacteria, parameterizing physiological processes and evaluating coefficients of the intertwined processes still remains challenging due in large extent to the lack of observations, especially for bacteria, in the oceans (e.g. Fasham et al. 1990, Luo et al. 2010).

Bacteria–phytoplankton interactions exist in a complex network of material exchanges. Different phytoplankton groups release DOC of different biochemical composition, molecular size, weight, and structure that confer varying degrees of DOC lability (Amon & Benner 1996, Hansell 2013). Non-motile bacteria have a relatively lower probability of encounter with phytoplankton-derived DOC and thus may not be immediately responsive to the gradient of DOC, while motile bacteria respond to DOC gradients immediately (Stocker 2012), which may result in more persistent coupling with phytoplankton. In nutrient limiting conditions, bacteria compete with phytoplankton for dissolved N and P while simultaneously remineralizing organic matter to N and P for phytoplankton (Wheeler & Kirchman 1986, Zweifel et al. 1993). Both bacteria and phytoplankton are under external physical forcing in the surrounding environment (e.g. temperature and irradiance), which may influence either or both of them. The principal link between phytoplankton and bacteria is the flux of DOC. For DOC, up to 5 different fractions are defined based on lifetimes and reactivity: labile DOC (LDOC), semi-labile DOC (SDOC), semi-refractory DOC (SRDOC), refractory DOC (RDOC), and ultra-refractory (URDOC) (Hansell 2013). More simply, DOC pools are usually grouped into 3 different fractions: LDOC (nanomolar concentration, turnover times of minutes to hours), SDOC (5–50 µM C, turnover times of days to months), and RDOC (30–40 µM C, turnover times of millennia) (Kirchman 2010). In the Sargasso Sea, and the open sea generally, nearly all DOC is ultimately derived from phytoplankton and its supply is further mediated by other food web processes. Typically, we only have estimates of the total bulk pool (~40–70 µM C at Bermuda), which does not respond directly to bacterial activity. The size of the semi-labile pool can be estimated by subtracting the deep water background (refractory) concentration from the total, or bulk pool. Measurements of the labile pool are not typically performed, but are becoming more common as analytical capabilities improve (Kujawinski 2011). The monthly sampling interval would lend little insight into the dynamics of the rapidly turning over labile pool. Here, we address the role of the semi-labile pool as a mechanism of coupling between phytoplankton and bacteria.

As a method for identifying causal associations in complex ecosystems, Sugihara et al. (2012) introduced convergent cross mapping (CCM) based on nonlinear state space reconstruction. Interactions among compartments within marine food webs are often difficult to analyze using conventional statistical approaches, such as cross-correlation, due to the ubiquity of weak and nonlinear coupling of such interactions which lead to changing signs of the correlations over different time periods tested (Casini et al. 2009, Sugihara et al. 2012). More importantly, correlation neither implies causality nor reveals the strength of a causal influence of one variable on another. CCM is an empirical modeling approach wherein a time series of interest can reveal its causal coupling with another. In recent years, CCM has been tested with a variety of time series, including relatively short ecological time series (Clark et al. 2015, Ye et al. 2015). Applying CCM to oceanic ecological time series provides a means to detect causal couplings among different biological processes apart from their covariability in the system.

In this study, we explored dynamic causal relationships between phytoplankton (i.e. primary production, PP) and heterotrophic bacteria (i.e. bacterial production, BP) by applying CCM. We analyzed the 24 yr time series of year-round monthly PP and BP observations from the Bermuda Atlantic Time-series Study (BATS) site in the North Atlantic Subtropical Gyre. We focused on this region because bacterial influence on phytoplankton might be significant compared to other regions especially during the summer stratification period when bacterial biomass can exceed that of the phytoplankton (Fuhrman et al. 1989). Our study aimed to (1) identify the causal influence of phytoplankton on bacteria and vice versa, (2) reveal the strength of causal influence in each direction, and (3) explore if bacterial–phytoplankton causal relationships depend on the physical regime. Here, we examined seasonal mixing as an example.

To our knowledge, this study is the first application of CCM to reveal the causality within microbial loop variables.

MATERIALS AND METHODS

BATS data extraction

Hydrography and ecosystem variables tested for CCM include mixed layer depth (MLD), PP via ^{14}C uptake, ^{3}H-thymidine (^{3}H-TdR) incorporation rates for calculating BP, and bulk DOC concentration, all obtained from the BATS database (http://batsftp.bios.edu/BATS/production/, http://batsftp.bios.edu/BATS/bottle/). MLD was calculated from the conductivity–temperature–depth (CTD) profiles using a finite difference temperature criterion ($\Delta T = 0.2°C$). Volumetric PP and ^{3}H-TdR incorporation rates were depth-integrated from the shallowest sample depth to the MLD using a trapezoidal method to represent upper mixed-layer inventories. For the purpose of CCM, we used depth-integrated values of each variable.

Conversions of phytoplankton and bacterial variables

Given that nitrate (NO_3^-) is a driver initiating seasonal phytoplankton dynamics at the BATS site, carbon PP estimates (mgC m^{-2} d^{-1}) were converted to nitrogen units (mmol N m^{-2} d^{-1}) using the canonical Redfield molar ratio for C:N of 6.625 (e.g. Fasham et al. 1990). We recognize that C:N ratio might change seasonally and thus as a function of the time periods we examined in this study, but it would not affect our results given that we worked with standardized monthly anomalies in the CCM (see below). Also for this reason, when necessary, we used DOC to get a more generalized picture of the processes linking bacteria and phytoplankton, rather than dissolved organic nitrogen or phosphorus. The MLD-integrated BP was derived from volumetric ^{3}H-TdR incorporation rates (pmol l^{-1} h^{-1}) using a formula by Carlson et al. (1996) and empirical conversion factors by Spitz et al. (2001) as follows:

$$BP = {}^{3}\text{H-TdR} \times \text{ICF} \times \text{biovolume} \times \text{CCF} \quad (1)$$

where ICF is an isotope conversion factor of 1.63×10^{18} cells mol^{-1}, biovolume is equivalent to 0.057 μm^3 $cell^{-1}$, and CCF is the carbon conversion factor of 120 fgC μm^{-3}. BP in carbon units was further converted to nitrogen units using bacterial C:N molar ratio of 4 (Caron et al. 1995).

Scientific justification for using CCM

In a linear stochastic system, future temporal evolution of the state is not determined from previous states but rather in a random manner. This type of system is governed by a high dimensional linear mode as a result of the additive action of many variables together (Hsieh et al. 2008). In a nonlinear dynamic system, future states follow from, or are unambiguously determined by, previous states where dynamics can be explained in a nonlinear mode by a few variables interacting in complicated ways (Hsieh et al. 2008). When a system is nonlinear, using linear statistical approaches (e.g. correlation) can lead to erroneous conclusions about 2 interacting variables in the system. Correlation might occur between the 2 variables in the absence of causation and causation might also occur in the absence of correlation. In other words, 2 biological variables might appear to causally impact each other, when they are not interacting, because they share common abiotic environments. Here, CCM allows us to tease out potential causal interaction between 2 biological variables from the effect of their shared environmental driver. CCM also enables us to examine directionality of such causal interactions (i.e. unidirectional or bidirectional causal influences). In our study, we tested a causal linkage between phytoplankton and bacteria, considering that their interactions might occur in a nonlinear dynamic manner (see below). Using CCM, a potential causal interaction between phytoplankton and bacteria can be revealed, as can the directionality of the causal influence between the 2 variables.

In nature, trophic interactions often show nonlinear and dynamic control or regime-dependent (i.e. top down versus bottom up) behaviors by which interactions between any 2 trophic levels are characterized by the changing sign of their correlation depending on a threshold value of another trophic level or an environmental forcing variable. For example, in the Baltic Sea ecosystem zooplankton population dynamics were dominantly driven more by either hydroclimatic forcing (bottom up) or predation pressure (top down) depending on the abundance threshold of a zooplanktivore. This suggests that a certain threshold of zooplanktivore abundance acts as a switch on bottom-up or top-down control on zooplankton dynamics (Casini et al. 2009). Here, we hypothesized that, as shown in the Baltic Sea ecosystem, phytoplankton and bacteria might show nonlinear behaviors and therefore their interactions would be best quantified if assumed in a nonlinear dynamic system,

rather than in a linear stochastic system, given the following reasoning. Ecologically, phytoplankton and bacteria interact via the flow of dissolved organic matter (DOM), where phytoplankton provide bacteria with DOM and bacteria feed on DOM for bacterial growth and biomass synthesis while remineralizing organic to inorganic nutrients for phytoplankton growth. Since bacterial activity is regulated by either temperature or DOM (phytoplankton-derived) availability or both in the ocean, a plausible hypothesis could be that a certain amount of biologically available DOM may switch on temperature control of bacteria, while DOM controls bacteria otherwise (i.e. DOM limitation/control vs. temperature limitation/control). Bearing in mind the possibility of nonlinear interactions between phytoplankton and bacteria at BATS, we tested if the BATS ecosystem is indeed a nonlinear dynamic system using an S-map algorithm (rEDM package; Chang et al. 2017). A nonlinear S-map model ($\theta > 0$) showed a better predictive skill than the linear S-map model ($\theta = 0$), confirming that the BATS ecosystem is best described as a nonlinear dynamic system (see Fig. S1 in the Supplement at www.int-res.com/articles/suppl/m600p041_supp.pdf). Therefore, CCM is a valid method to best reveal the interactions between phytoplankton and bacteria at BATS.

CCM algorithm

The CCM algorithm is based on state space reconstruction with a lagged coordinate embedding of time series data (Takens 1981). In a nonlinear deterministic system, there is an underlying coherent trajectory called a manifold governing the dynamics, and it is said that 2 variables are causally linked if they share a common attractor manifold $\boldsymbol{M}$ (Sugihara et al. 2012). When causally coupled, each variable can identify the state of the other. The basic principle of CCM is that information about a causal variable is recorded in the affected variable and that this link can be confirmed by cross-prediction, i.e. when the former can be estimated using the temporal sequence of the latter with the CCM algorithm (Sugihara & May 1990, Sugihara et al. 2012). The causal links between bacteria and phytoplankton can be established by assuming the 2 variables are alternative observations of a common attractor manifold $\boldsymbol{M}$. To the extent this holds true, data on bacteria and phytoplankton can approximate the state of each other when provided with suitable time lags. For example, the causal effect of bacteria on phytoplankton is detected by measuring the extent to which the past record of the phytoplankton provides a reliable estimate of the states of the bacteria. The CCM algorithm detects a signature of bacteria (X hereafter) in phytoplankton (Y hereafter) based on a correspondence between the 2 attractor manifolds, $\boldsymbol{M_X}$ and $\boldsymbol{M_Y}$, which are E (size of embedding dimension) padded temporal sequences of bacteria and phytoplankton, respectively. For further details of CCM algorithms and equations, see Supplementary Material page 4 in Sugihara et al. (2012).

In a brief description of the CCM algorithm, consider a data library of 2 variables of length L, $\{X\} = \{X(1), X(2), \ldots, X(L)\}$ and $\{Y\} = \{Y(1), Y(2), \ldots, Y(L)\}$ and a shadow manifold $\boldsymbol{M_Y}$ which consists of lagged-coordinate vectors $y(t) = <Y(t), Y(t-\tau), \ldots, Y(t-(E-1)\tau)>$, with τ time interval and $\boldsymbol{M_X}$ of $x(t)$. Note that the contemporaneous $y(t^*)$ and $x(t^*)$ at time of t^* are excluded from the library to form an attractor manifold. By locating the contemporaneous $y(t^*)$ on $\boldsymbol{M_Y}$ to find its $E+1$ nearest neighbors and identifying the $E+1$ putative neighbors of $x(t^*)$ in $\{X\}$, the contemporaneous $X(t^*)$ is estimated from a locally weighted mean as follows:

$$\hat{X}\Big|\boldsymbol{M}_Y = \sum_{i=1}^{E+1} w_i X(t_i) \tag{2}$$

where w_i is a weighting based on the distance between $\underline{y}(t)$ (i.e. the vector on $\boldsymbol{M_Y}$ corresponding to the state of the system at time t) and its ith nearest neighbor on $\boldsymbol{M_Y}$, and $X(t_i)$ are the contemporaneous values of X. The weights, w_i, are calculated as follows:

$$w_i = u_i \Big/ \sum_{j=1}^{E+1} u_j \tag{3}$$

where

$$u_i = e^{-\mathrm{d}[\underline{y}(t),\underline{y}(t_i)]/\mathrm{d}[\underline{y}(t),\underline{y}(t_1)]} \tag{4}$$

and where $\mathrm{d}[\underline{y}(s), \underline{y}(t)]$ is the Euclidean distance between 2 vectors. If causality is detected, the correlation (rho, ρ) between the actual data and the estimation improves and converges as the size of the data library increases.

For CCM, we used standardized monthly anomalies of each variable to reduce the confounding effects of seasonal cycle (Fig. 1). Standardized monthly anomalies were calculated by removing monthly climatology (mean) from data values and then dividing them by monthly standard deviation. The detection of causality of X (or Y) on Y (or X) is based on 2 criteria: (1) when the correlation (ρ) between the cross-mapped estimate and actual value is greater with the largest library than with the smallest library (i.e. L,

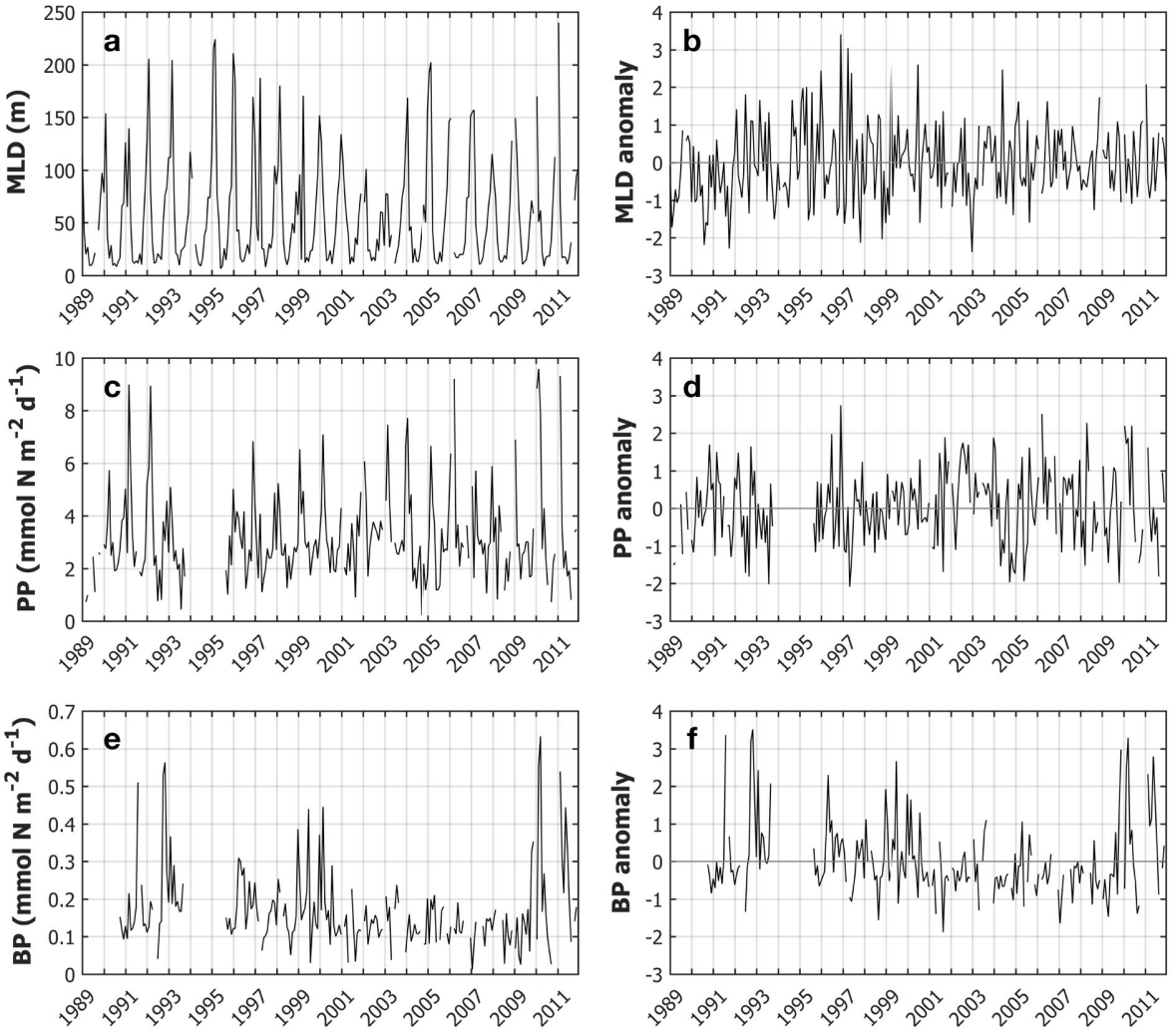

Fig. 1. Time series of mixed layer depth (MLD), primary production (PP), and bacterial production (BP) used for convergent cross mapping (CCM) in this study. (a,c,e) Monthly means and (b,d,f) standardized monthly anomalies of MLD, PP, and BP

the number of all data points entered in the CCM models) and (2) when ρ > 0 at the longest *L* (Clark et al. 2015). For example, Fig. S2 shows the correlation between the reconstructed bacterial values and actual bacterial values as a function of library size. For our CCM models, we chose $E = 3$ as our embedding dimension time lag given that (1) auto-correlation of the underlying monthly time series variables in our study decreases considerably after 1–2 mo and (2) $E = 3$ produced the best predictive skill in the CCM models among varying *E* tested ($E = 2–7$). To ensure the robustness of our CCM results, we performed leave-one-out cross validation where the CCM model was repeatedly performed leaving out a single year's dataset (i.e. a verification year) and then used to derive a prediction for the left-out observation (i.e. library years). In order to determine statistical significance of the detected causality, we first generated the randomized time series from the original time series. Next, we carried out randomization on the standardized monthly anomalies of each variable by preserving the range of the distribution to that of the original time series (i.e. multiplying each randomized value by the maximum range, i.e. maximum minus minimum, of the original time series). CCM was then repeatedly performed to simulate a series of Monte Carlo experiments ($m = 30$) with the randomized time series within the ranges of the original time series. This way, ρ in the CCM results above the error shading from Monte Carlo simulations is considered statistically significant. In some cases, ρ is above the range of Monte Carlo-generated errors but shows lack of convergence, which we interpreted as lack of causality, since in this case the

CCM model is not yet stabilized with the given length of the time series (e.g. the [non]causality of phytoplankton on bacteria during the stratification period).

To ensure that our CCM algorithm works properly, we first employed our CCM algorithm to synthetic data generated from known equations which dictate unidirectional causal forcing of *X* on *Y*, while the dynamics of *X* are not influenced by those of *Y* but rather predicted simply by its own previous time step (Fig. S3). To test the performance of our CCM with the time series of variables tested for the present study, we also applied CCM to synthetic time series output produced from the Fasham-Ducklow-McKelvie (FDM, Fasham et al. 1990) model (see below) for which unidirectional coupling is anticipated (e.g. causality between MLD and phytoplankton; Fig. S4). We then applied our CCM algorithm to the BATS observational data sets, again with MLD and phytoplankton (Fig. S5). In addition to testing the validity of grouping into different seasonal mixing time frames (see below), this procedure enables us to examine how the presumed patterns of causality between the 2 field observational variables might be affected by observational noise and sampling errors. In all 3 cases, the directions of the causality between the tested variables were correctly recovered, providing confidence and robustness in applying our CCM algorithm to the variables explored in this study.

FDM ecosystem model

The FDM model is a time-dependent box model with 7 foodweb compartments in an upper-ocean mixed layer dictated by coupled ordinary differential equations (Fasham et al. 1990). The model compartments include nitrate, phytoplankton, zooplankton, bacteria, ammonium (NH_4^+), dissolved organic nitrogen, and detritus. The equations for model constituents are described by Fasham et al. (1990). Many ecologists have modified the FDM model mostly by adding size-fractionated plankton as additional compartments; however, we used the original version of the FDM model since the variables of interest (PP and BP) for CCM in our study are bulk variables which represent entire microbial assemblages. Whereas previous studies used the FDM model to explore steady-state solutions, we used the FDM model to produce time-varying data by applying 55 yr long historical records of monthly mean MLD and cloud fraction from Ocean Reanalysis System 4 (ORAS4) and ERA-20C data sets (www.ecmwf.int/en/research/climate-reanalysis), respectively.

Defining the mixing regimes

The dynamics of physical mixing in the Sargasso Sea differ considerably between the winter–spring mixing period (November to April; from the month when the MLD first crosses the nitracline to the next 6 mo) and the summer–fall stratification period (May to October) (Fig. 2). During the mixing period, nitrate is entrained into the euphotic zone by wind-driven mixing, whereas during the stratification period, nitrate supply is mostly limited to diffusional inputs unless episodic summertime storms induce mixing events (Moore et al. 2008). The 2 different seasonal mixing regimes are also characterized by distinct microorganisms dominating the phytoplankton. During the winter mixing period, picoeukaryotes and *Synechococcus,* resistant to mixing-induced photoinactivation (Mella-Flores et al. 2012), often dominate in winter–spring phytoplankton blooms (DuRand et al. 2001, Moore et al. 2008). During the summer stratification period, *Prochlorococcus* dominates in the phytoplankton due to its ability to use regenerated NH_4^+ from *Trichodesmium* and other

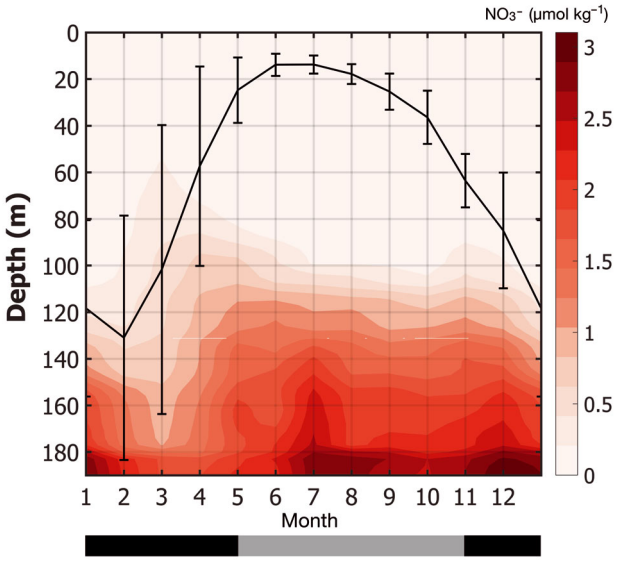

Fig. 2. Climatology (1989–2012) of mixed layer depth (MLD) overlaid on nitrate (NO_3^-) concentration (µmol kg^{-1}) in the water column. Error bars indicate standard deviation. The black shaded area indicates the winter–spring mixing period and the grey shaded area represents the summer–fall stratification period

species (DuRand et al. 2001, Hood et al. 2001, Boushaba & Pascual 2005, Moore et al. 2008, Malmstrom et al. 2010, Casey et al. 2013, Wallhead et al. 2014).

Based on the distinct seasonal microbial dynamics dictated by different seasonal mixing regimes, we hypothesized that causal relationships between phytoplankton and bacteria differ seasonally. First, in the beginning of the winter–spring mixing period, a deepening of the MLD and resultant entrainment of nitrate into the euphotic zone drive phytoplankton growth, which may induce the causality of phytoplankton on bacteria via bacterial growth from an increase in the phytoplankton-derived SDOC pool (Carlson et al. 1994, 1996, Michaels et al. 1994, Michaels & Knap 1996, Steinberg et al. 2001). In the summer–fall stratification period, phytoplankton growth is highly limited due to minimal diffusive nitrate input in the upper mixed layer, and phytoplankton rely mostly on regenerated nitrogen. We hypothesized that this would show the causality of bacteria on phytoplankton during the stratification period. Thus, we grouped the time periods for testing CCM into the mixing period (November–April) and the stratification period (May–October) which represent 2 seasonally driven, distinct physical mixing regimes.

As addressed in the Introduction, we note that variations in the total bulk DOC pool are not sensitive to the short-term BP rates, and vice versa. Thus, phytoplankton causality on bacteria may be obscured by this limitation. The majority of the bulk DOC is refractory, with constant concentration over time. Thus, temporal fluctuation of the bulk DOC is driven by the semi-labile pool. Hereafter, we only consider SDOC in the analysis by subtracting the background concentration for RDOC (42 µM C at BATS) from bulk DOC concentrations. Technically, these data include the labile pool but its dynamics are not resolved by our measurements. We also recognize that the semi-labile and total bulk pools are mathematically equivalent. For this reason, we use SDOC instead of DOC throughout this manuscript.

RESULTS

Phytoplankton–bacterial causality during the mixing period

During the mixing period, we did not detect a causal impact of phytoplankton on bacteria, nor of bacteria on phytoplankton. The results from both cases did not meet the criteria of causality (see 'Materials and methods: CCM algorithm') showing that ρ was consistently <0 when library size increased (Fig. 3a,b). Cross-correlation between phytoplankton and bacterial anomalies during the mixing period also revealed no coupling (r =

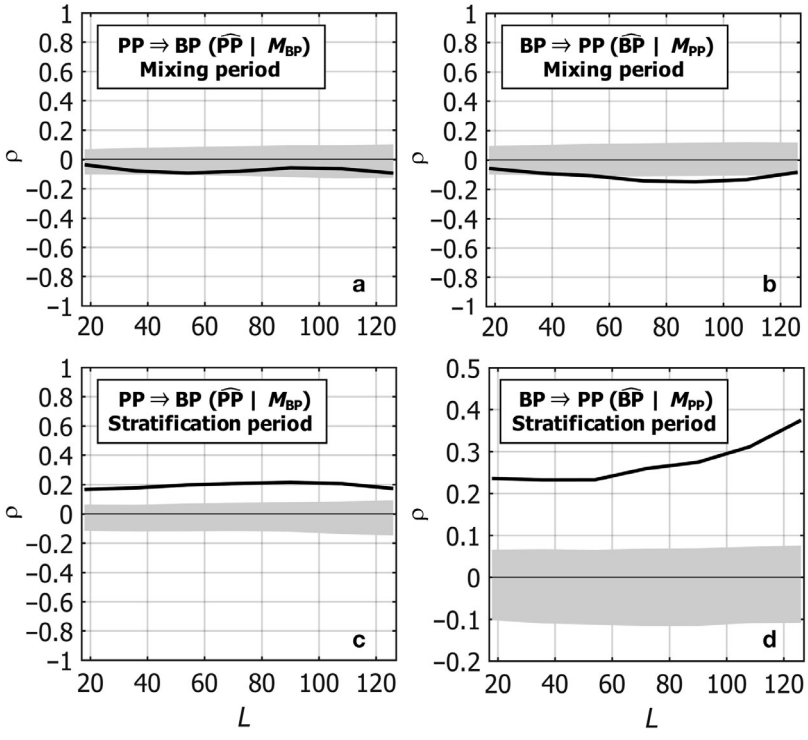

Fig. 3. Detecting causality between phytoplankton (primary production, PP) and bacteria (bacterial production, BP) during the 2 different physical mixing regimes using convergent cross mapping (CCM). PP and BP rates are integrated from surface to mixed layer depth (MLD). For CCM, standardized monthly anomalies of PP and BP (Fig. 1) were used. The arrow above each plot indicates the direction of a causal influence of one variable on another variable, where PP ⇒ BP indicates the causality of PP on BP (i.e. $\widehat{PP} \mid \boldsymbol{M}_{BP}$). The shaded area represents error spread or confidence intervals (5%–95%) generated from Monte Carlo simulations (n = 30). The detection of causality for the given directional flow was established based on the signature of convergence from library size (*L*) versus Pearson correlation coefficient (ρ) where (1) ρ converges to a value of significantly >0 as *L* increases and (2) ρ is greater at the longest *L*. According to these criteria, there was (a) no phytoplankton causality on bacteria during the mixing period, (b) no bacterial causality on phytoplankton during the mixing period, (c) no phytoplankton causality on bacteria during the stratification period, and (d) moderate bacterial causality on phytoplankton during the stratification period

0.14, p = 0.15), so absence of causal association was correctly inferred from cross-correlation during this time period. To gain insight into why causality was absent between phytoplankton and bacteria, we examined depth-integrated composites of nitrate, particulate organic carbon (POC), SDOC, and BP within the MLD (Fig. 4). In response to deeper mixing (i.e. positive MLD anomalies), NO_3^- (Fig. 4a), POC (Fig. 4b), and SDOC (Fig. 4c) all significantly increased. Despite increased availability of phytoplankton-derived organic carbon pools, BP (Fig. 4d) did not increase as a result of deeper mixing. To understand a complete picture of the phytoplankton–bacterial causal dynamics, which should ultimately include SDOC as a mediator variable, we additionally examined the causality of PP on SDOC, as well as the causality of SDOC on BP. However, no signals of the causality were detected in either case (Fig. S6a,b).

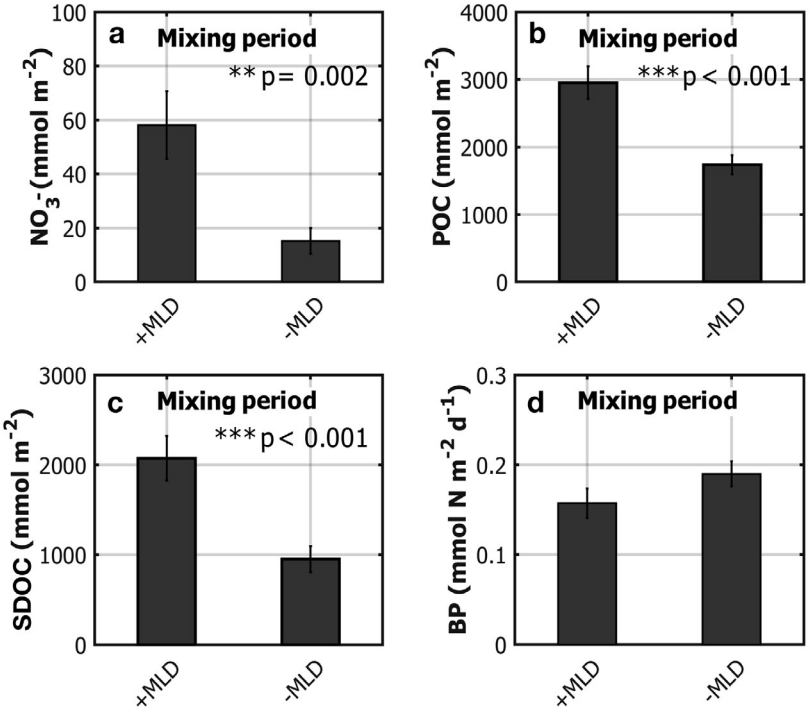

Fig. 4. Ecosystem (nitrate, particulate organic carbon [POC], semi-labile dissolved organic carbon [SDOC], and bacterial production [BP]) composites during positive mixed layer depth (MLD; i.e. deeper mixing) and negative MLD (i.e. shallower mixing) anomaly months during 2 different seasonal mixing regimes. Here, SDOC is the sum of the semi-labile and labile DOC pools (i.e. bulk DOC minus refractory background concentration of 39 µM C at the Bermuda Atlantic Time-series Study [BATS] site). +MLD (–MLD) indicates positive (negative) MLD anomalies. Significance of difference between positive and negative MLD anomaly months was determined by Student's *t*-test at $p < 0.05$. Error bars indicate standard errors

Phytoplankton–bacterial causality during the stratification period

In contrast to the mixing period, the stratification period was characterized by a unidirectional causal relationship of bacteria on phytoplankton, while the causality of phytoplankton on bacteria seemed yet unclear (Fig. 3c,d). Cross-correlation between PP and BP during the stratification period also showed a significant and moderate coupling between them (r = 0.44, p < 0.001). However, importantly, our CCM suggests that the observed coupling was actually driven by bacterial causality on phytoplankton, not vice versa, which would not be revealed by cross-correlation alone. As done for the mixing period, we tested the causality of phytoplankton on SDOC and the causality of SDOC on bacteria during the stratification period as well. There was no signal of the causal influence of phytoplankton on SDOC (Fig. S6c). However, strong causality was detected in the flow from SDOC to bacteria (Fig. S6d).

DISCUSSION

Phytoplankton–bacterial causality during the mixing period

The lack of bi-directional causality between phytoplankton and bacteria (Fig. 5a) contradicts our initial expectation of a causal impact of phytoplankton on bacteria during the mixing period, which was based upon observations that an increase in phytoplankton productivity from mixing and nitrate entrainment supplies bacteria with organic carbon sources (Carlson et al. 1994, 1996, Michaels et al. 1994, Michaels & Knap 1996, Steinberg et al. 2001). The lack of bacterial causality on phytoplankton during the mixing period is easier to understand because phytoplankton growth during this period is mostly supported by newly introduced nitrate from winter mixing rather than by recycled nutrients from bacterial remineralization (Fasham et al. 1990, Siegel et al. 1999, Lipschultz 2001). Considering that most of phytoplankton-derived carbon is

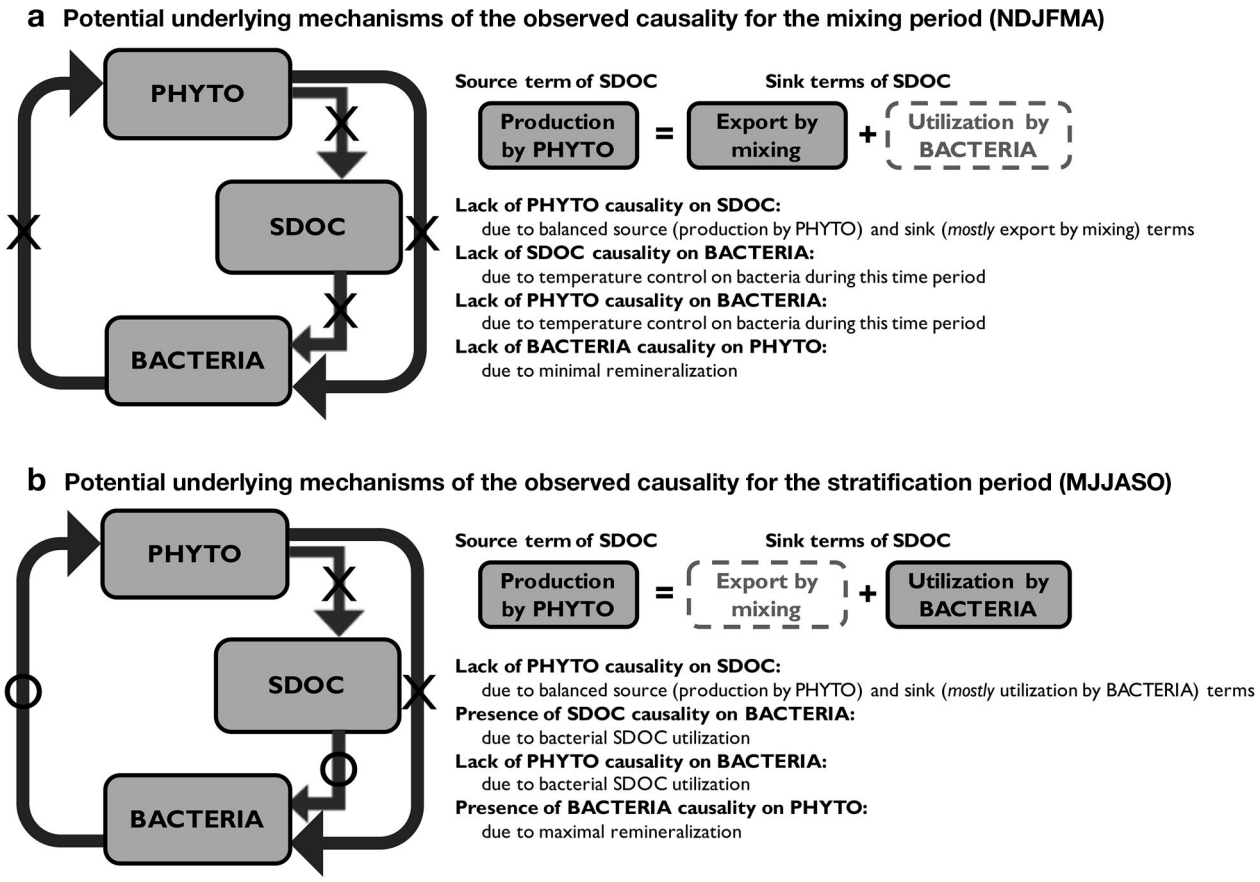

Fig. 5. Summary of mixing regime-dependent causality between phytoplankton and bacteria via semi-labile dissolved organic carbon (SDOC) as a mediator. 'O' indicates a causal influence of one variable on another and 'X' indicates the lack of a causal influence of one variable on another in the given direction of the flow based on the results of convergent cross mapping (CCM) in Fig. 3. PHYTO: phytoplankton

routed through SDOC in the Sargasso Sea (Carlson et al. 1998), we tested the causality of phytoplankton on SDOC as well as the causality of SDOC on bacteria to gain mechanistic insight into the lack of phytoplankton causality on bacteria. However, there was no evidence of the causality in either case during the mixing period.

During the mixing period at BATS, deep mixing of the water column acts as a direct removal process (sink) for SDOC because SDOC accumulated since previous seasons is exported to the sub-euphotic zone as a result of winter mixing (Hansell & Carlson 2001). Similarly, bacterial utilization, if integrated over days to months as in our study, could also function as a sink for SDOC (bearing in mind that actual BP measurements made over hours largely reflect the uptake of LDOC but strictly speaking, the amount of SDOC uptake remains unknown). By contrast, winter mixing leads to entrainment of nitrate into the upper euphotic zone and subsequently to larger phytoplankton productivity, accumulation, and SDOC stock in the upper mixed layer (Carlson et al. 1994, 1998, Hansell & Carlson 1998), which was also evidenced by our results (Fig. 4a–c). In this aspect, mixing acts as an indirect source of SDOC via increased production. Our observation of the lack of phytoplankton causality on SDOC suggests that during the mixing period, there were balanced source (via phytoplankton production) and sink (via export and bacterial utilization) terms for SDOC (Fig. 5a). However, it should be noted that in contrast to deeper mixing-induced increases in POC and SDOC stocks (Fig. 4a), BP did not show a corresponding enhancement in more deeply mixed water columns (Fig. 4d). For this, our recent findings at BATS demonstrated that BP was inhibited significantly in more deeply mixed water columns due to deep mixing-induced entrainment of cold water into the upper mixed layer; during the winter mixing period, BP was strongly controlled by temperature and was not limited by SDOC availability (Fig. S7). This observation rules out increased bacterial SDOC utilization as

the reason for larger SDOC removal during deeper mixing; rather, it more likely stems from increased SDOC export out of the upper euphotic zone by deeper mixing. This observation also provides a mechanistic basis for the lack of SDOC causality on bacteria as well as for the lack of phytoplankton causality on bacteria during the mixing period (Fig. 5a). Based on these findings, we propose cold water entrainment and the resulting inhibition of BP as a potential underlying mechanism of the lack of phytoplankton causality on bacteria during the mixing period.

Another possible explanation for the lack of phytoplankton causality on SDOC would be that SDOC variability is also caused by other intermediate food web processes (e.g. zooplankton sloppy feeding and viral lysis) for which quantification is beyond the scope of our study. Even if this is the case, it reformulates the potential underlying mechanisms neither for the lack of SDOC causality on bacteria nor for the lack of phytoplankton causality on bacteria.

Phytoplankton–bacterial causality during the stratification period

The result of the moderate degree of unidirectional bacterial causality on phytoplankton (Fig. 5b) is consistent with our hypothesis that bacterial variability might significantly cause phytoplankton variability, hypothetically because bacteria directly provide regenerated nutrients such as NH_4^+ during the summer–fall stratification period. Relatively speaking, explaining the lack of causality of phytoplankton on bacteria is more complicated. At first glance, the strong SDOC causality on bacteria may seem puzzling as there is no causal influence of phytoplankton on SDOC during the stratification period.

During the stratification period at BATS, not much organic carbon comes from phytoplankton-derived fresh and labile carbon due to very limited phytoplankton activity as a result of reduced mixing of the water column (Lipschultz 2001). The carbon accumulated in surface waters during this period is semi-labile and shows very little temporal fluctuation during the stratification period (Carlson et al. 2002, 2004). Our observation of the lack of phytoplankton causality on SDOC implies that SDOC is in a rough steady state with balanced production (via phytoplankton) and removal (via export and bacterial utilization). Given that SDOC removal by mixing-induced export is low during the stratification period, bacterial utilization should account for most of the SDOC removal. Thus, the lack of phytoplankton causality on SDOC indicates that SDOC produced by phytoplankton is balanced by SDOC utilization by bacteria (Fig. 5b). In other words, it might be the case that bacteria utilize SDOC in surface waters during the stratification period. The lack of phytoplankton causality on bacteria but with the presence of SDOC causality on bacteria implies that other foodweb processes may also contribute to SDOC variability during the stratification period (Fig. 5b). Given that cold temperature no longer played a role in inhibiting bacterial activity during warm stratification periods, bacterial activity might be significantly limited by SDOC availability (i.e. more SDOC leads to higher BP). Based on these findings, our CCM results challenge previous observations at BATS that did not show surface bacterial SDOC utilization with a resolution of the measurement (Carlson et al. 2002, 2004). However, there is evidence that bacteria in the surface layer could encounter conditions allowing SDOC to be used. Though limited, episodic mixing events could bring subsurface bacteria capable of using SDOC into the surface layer (Carlson et al. 2004). Bacterial utilization of SDOC might be aided by photo-decomposition of SDOC to more labile forms (Kieber et al. 1989, McCallister et al. 2005, Collins 2017). Carlson et al. (2009) showed that SAR11 ecotypes II and Ib, which are suggested to be capable of remineralizing euphotic zone-produced SDOC, were found in surface waters at BATS during the stratification period.

Other ecological considerations

While our findings are novel as the first attempt to reveal the bidirectional causal associations between the 2 major components in the microbial loop, there are important analytical and data-related uncertainties. Similar to the complementary tests on SDOC we performed, it is critical to test causal relationships with NH_4^+, given that ammonium is the principal inorganic nutrient regenerated by bacteria and supporting phytoplankton activity, especially during the stratification period. However, ammonium data are not available from the BATS site. The FDM model has an ammonium compartment, but without actual field observations at BATS, it is impossible to constrain the model to simulate realistic ammonium dynamics. Besides, the recently modified FDM model showed that an almost equivalent amount of ammonium comes from zooplankton as compared to heterotrophic bacteria (Spitz et al. 2001), which might

obscure the causality of bacteria on NH_4^+. There might be biological process-oriented sources of uncertainties in our CCM results. Microbially, the BATS region is a seasonally dynamic ecosystem showing evidence of significant nitrogen fixation by photoautotrophic nitrogen-fixing bacteria, which do not contribute to (heterotrophic) BP rates tested for CCM in our study (i.e. they do not use exogenously supplied thymidine). Diazotroph species like *Trichodesmium* contribute to new production by nitrogen fixation during the stratification period, triggering occasional outbursts of diatoms without mixing-induced entrainment of new nitrogen as a prerequisite (Orcutt et al. 2001, Lipschultz et al. 2002). With regard to CCM, nitrogen fixation during the stratification period has the potential to weaken the causality of bacteria on phytoplankton. Nonetheless, our results demonstrate the moderate strength of bacterial causality on phytoplankton during the stratification period, implying a mathematically minor effect of this nitrogen cycling bacterial group at BATS. Hansell & Carlson (2001) suggested that nitrogen fixation is minimal during the summer stratification period at BATS as inferred from no substantial increase in total organic nitrogen (TON), unlike large increases in TON pools in the presence of nitrogen fixers *Trichodesmium* at Station ALOHA in the North Pacific (Karl et al. 1992). Lastly, it should be noted that our analysis only considered bacterial values within the MLD, but bacterial maxima are typically formed at depths (i.e. 50–60 m) deeper than the mixed layer in the stratification period (Steinberg et al. 2001). It is yet unclear how taking these BP maximum layers into account would change the observed causal relationships among the microbial loop variables examined in our study.

CONCLUSIONS

The findings of our study highlight physical mixing regime-dependent causal relationships between phytoplankton and bacteria (Fig. 5). The causal associations between phytoplankton and bacteria were absent in both directions during the mixing period (Fig. 5a). During the winter–spring mixing period, the lack of the causality of phytoplankton on bacteria might be explained by bacterial inhibition from mixing-induced cold water entrainment into the upper euphotic zone despite plenty of SDOC availability (Fig. S7). The lack of causality of bacteria on phytoplankton might be due to predominant phytoplankton utilization of newly introduced nitrate from mixing, rather than on regenerated nutrients via bacteria (Siegel et al. 1999, Lipschultz 2001). In contrast, the stratification period was characterized by a moderate degree of bacterial causality on phytoplankton (Fig. 5b) that is presumably due to phytoplankton utilization of regenerated ammonium via bacterial remineralization (Lipschultz 2001). The causal influence of phytoplankton on bacteria was absent during the stratification period, possibly as a result of bacterial utilization of SDOC. Significant bacterial utilization of SDOC might also be inferred from the strong SDOC causality on bacteria. These findings suggest bacterial utilization of SDOC during the stratification period.

Modeling ecosystem dynamics is a challenging task due to our incomplete understanding of underlying processes, the regime-dependent behavior of microorganisms, and the shortage of real field measurements of essential parameters and coefficients in the specific physiological processes required to tune model fits to observations. Using this empirical approach for revealing causality, our study successfully addresses that causal associations among microbially important processes can be revealed in a data-driven manner, thereby promoting our understanding of further impacts on carbon fluxes, cycling, and sequestration in the oceans via the microbial loop.

Acknowledgements. We thank the many current and former scientists at the Bermuda Institute of Ocean Sciences for field sampling, processing, and analyses. We also thank George Sugihara and Scott Doney for their helpful comments on this manuscript. Support for H.K. came from the Department of Earth and Environmental Sciences at Columbia University and a subcontract to Lamont-Doherty Earth Observatory (LDEO) from NASA ROSES award NNX14AL86G to Scott Doney at Woods Hole Oceanographic Institution (now at the University of Virginia). D.E.L. was supported by the Office of Naval Research under Grant No. N00014-12-1-0911. H.W.D. was supported in part by a gift from the Vetleson Foundation to LDEO.

LITERATURE CITED

Amon RM, Benner R (1996) Bacterial utilization of different size classes of dissolved organic matter. Limnol Oceanogr 41:41–51

Azam F, Fenchel T, Field JG, Gray JS, Meyer-Reil LA, Thingstad F (1983) The ecological role of water-column microbes in the sea. Mar Ecol Prog Ser 10:257–263

Boushaba K, Pascual M (2005) Dynamics of the 'echo' effect in a phytoplankton system with nitrogen fixation. Bull Math Biol 67:487–507

Carlson CA, Ducklow HW, Michaels AF (1994) Annual flux of dissolved organic carbon from the euphotic zone in the northwestern Sargasso Sea. Nature 371:405–408

Carlson CA, Ducklow HW, Sleeter TD (1996) Stocks and

dynamics of bacterioplankton in the northwestern Sargasso Sea. Deep-Sea Res II 43:491–515
Carlson CA, Ducklow HW, Hansel DA (1998) Organic carbon partitioning during spring phytoplankton blooms in the Ross Sea polynya and the Sargasso Sea. Limnol Oceanogr 43:375–386
Carlson CA, Giovannoni SJ, Hansell DA, Goldberg SJ and others (2002) Effect of nutrient amendments on bacterioplankton production, community structure, and DOC utilization in the northwestern Sargasso Sea. Aquat Microb Ecol 30:19–36
Carlson CA, Giovannoni SJ, Hansell DA, Goldberg SJ, Parsons R, Vergin K (2004) Interactions among dissolved organic carbon, microbial processes, and community structure in the mesopelagic zone of the northwestern Sargasso Sea. Limnol Oceanogr 49:1073–1083
Carlson CA, Morris R, Parsons R, Treusch AH, Giovannoni SJ, Vergin K (2009) Seasonal dynamics of SAR11 populations in the euphotic and mesopelagic zones of the northwestern Sargasso Sea. ISME J 3:283–295
Caron DA, Dam HG, Kremer P, Lessard EJ, Madin LP, Malone TC, Youngbluth MJ (1995) The contribution of microorganisms to particulate carbon and nitrogen in surface waters of the Sargasso Sea near Bermuda. Deep-Sea Res I 42:943–972
Casey JR, Aucan JP, Goldberg SR, Lomas MW (2013) Changes in partitioning of carbon amongst photosynthetic pico-and nano-plankton groups in the Sargasso Sea in response to changes in the North Atlantic Oscillation. Deep-Sea Res II 93:58–70
Casini M, Hjelm J, Molinero JC, Lövgren J and others (2009) Trophic cascades promote threshold-like shifts in pelagic marine ecosystems. Proc Natl Acad Sci USA 106:197–202
Chang CW, Ushio M, Hsieh CH (2017) Empirical dynamic modeling for beginners. Ecol Res 32:785–796
Clark AT, Ye H, Isbell F, Deyle ER, Cowles J, Tilman GD, Sugihara G (2015) Spatial convergent cross mapping to detect causal relationships from short time series. Ecology 96:1174–1181
Cole JJ, Findlay S, Pace ML (1988) Bacterial production in fresh and saltwater ecosystems: a cross-system overview. Mar Ecol Prog Ser 43:1–10
Collins JR (2017) The remineralization of marine organic matter by diverse biological and abiotic processes. PhD dissertation, Massachusetts Institute of Technology, Cambridge, MA
DuRand MD, Olson RJ, Chisholm SW (2001) Phytoplankton population dynamics at the Bermuda Atlantic Time-series station in the Sargasso Sea. Deep-Sea Res II 48: 1983–2003
Fasham M, Ducklow H, McKelvie SM (1990) A nitrogen-based model of plankton dynamics in the oceanic mixed layer. J Mar Res 48:591–639
Fuhrman JA, Sleeter TD, Carlson CA, Proctor LM (1989) Dominance of bacterial biomass in the Sargasso Sea and its ecological implications. Mar Ecol Prog Ser 57:207–217
Hansell DA (2013) Recalcitrant dissolved organic carbon fractions. Annu Rev Mar Sci 5:421–445
Hansell DA, Carlson CA (1998) Net community production of dissolved organic carbon. Global Biogeochem Cycles 12:443–453
Hansell DA, Carlson CA (2001) Biogeochemistry of total organic carbon and nitrogen in the Sargasso Sea: control by convective overturn. Deep-Sea Res II 48:1649–1667
Hood RR, Bates NR, Capone DG, Olson DB (2001) Modeling the effect of nitrogen fixation on carbon and nitrogen fluxes at BATS. Deep-Sea Res II 48:1609–1648
Hsieh CH, Anderson C, Sugihara G (2008) Extending nonlinear analysis to short ecological time series. Am Nat 171:71–80
Karl DM, Letelier R, Hebel DV, Bird DF, Winn CD (1992) *Trichodesmium* blooms and new nitrogen in the North Pacific gyre. In: Carpenter EJ, Capone DG, Rueter JG (eds) Marine pelagic cyanobacteria: *Trichodesmium* and other diazotrophs. Springer, Dordrecht, p 219–237
Kieber DJ, McDaniel J, Mopper K (1989) Photochemical source of biological substrates in seawater: implications for carbon cycling. Nature 341:637–639
Kirchman DL (2010) Microbial ecology of the oceans (Vol 36). John Wiley & Sons, Hoboken, NJ
Kujawinski EB (2011) The impact of microbial metabolism on marine dissolved organic matter. Annu Rev Mar Sci 3: 567–599
Legendre L, Le Fèvre J (1991) From individual plankton cells to pelagic marine ecosystems and to global biogeochemical cycles. In: Demers S (ed) Particle analysis in oceanography. Springer-Verlag, Berlin, p 261–299
Lipschultz F (2001) A time series assessment of the nitrogen cycle at BATS. Deep-Sea Res II 48:1897–1924
Lipschultz F, Bates NR, Carlson CA, Hansell DA (2002) New production in the Sargasso Sea: history and current status. Global Biogeochem Cycles 16:1001
Luo YW, Friedrichs MAM, Doney SC, Church MJ, Ducklow HW (2010) Oceanic heterotrophic bacterial nutrition by semilabile DOM as revealed by data assimilative modeling. Aquat Microb Ecol 60:273–287
Malmstrom RR, Coe A, Kettler GC, Martiny AC, Frias-Lopez J, Zinser ER, Chisholm SW (2010) Temporal dynamics of *Prochlorococcus* ecotypes in the Atlantic and Pacific oceans. ISME J 4:1252–1264
McCallister SL, Bauer JE, Kelly J, Ducklow HW (2005) Effects of sunlight on decomposition of estuarine dissolved organic C, N and P and bacterial metabolism. Aquat Microb Ecol 40:25–35
Mella-Flores D, Six C, Ratin M, Partensky F, Boutte C, Le Corguille G, Garczarek L (2012) *Prochlorococcus* and *Synechococcus* have evolved different adaptive mechanisms to cope with light and UV stress. Front Microbiol 3: 285
Michaels AF, Knap AH (1996) Overview of the U.S. JGOFS Bermuda Atlantic Time-series Study and the Hydrostation S program. Deep-Sea Res II 43:157–198
Michaels AF, Knap AH, Dow RL, Gundersen K and others (1994) Seasonal patterns of ocean biogeochemistry at the US JGOFS Bermuda Atlantic Time-series Study site. Deep-Sea Res I 41:1013–1038
Moore CM, Mills MM, Langlois R, Milne A, Achterberg EP, LaRoche J, Geider RJ (2008) Relative influence of nitrogen and phosphorous availability on phytoplankton physiology and productivity in the oligotrophic subtropical North Atlantic Ocean. Limnol Oceanogr 53: 291–305
Orcutt KM, Lipschultz F, Gundersen K, Arimoto R, Gallon JR, Michaels AF, Knap AH (2001) Seasonal pattern and significance of N fixation by *Trichodesmium* at the Bermuda Atlantic Time-series Study (BATS) site. Deep-Sea Res II 48:1583–1608
Pomeroy LR (1974) The ocean's food web, a changing paradigm. BioScience 24:499–504
Sañudo-Wilhelmy SA, Gómez-Consarnau L, Suffridge C,

Webb EA (2014) The role of B vitamins in marine biogeochemistry. Annu Rev Mar Sci 6:339–367
Siegel DA, McGillicuddy DJ Jr, Fields EA (1999) Mesoscale eddies, satellite altimetry, and new production in the Sargasso Sea. J Geophys Res 104:13359–13379
Siegel DA, Buesseler KO, Behrenfeld MJ, Benitez-Nelson CR and others (2016) Prediction of the export and fate of global ocean net primary production: the EXPORTS science plan. Front Mar Sci 3:22
Spitz YH, Moisan JR, Abbott MR (2001) Configuring an ecosystem model using data from the Bermuda Atlantic Time Series (BATS). Deep-Sea Res II 48:1733–1768
Steinberg DK, Carlson CA, Bates NR, Johnson RJ, Michaels AF, Knap AH (2001) Overview of the US JGOFS Bermuda Atlantic Time-series Study (BATS): a decade-scale look at ocean biology and biogeochemistry. Deep-Sea Res II 48:1405–1447
Stocker R (2012) Marine microbes see a sea of gradients. Science 338:628–633
Sugihara G, May RM (1990) Nonlinear forecasting as a way of distinguishing chaos from measurement error in time series. Nature 344:734–741
Sugihara G, May R, Ye H, Hsieh CH, Deyle E, Fogarty M, Munch S (2012) Detecting causality in complex ecosystems. Science 338:496–500
Takens F (1981) Detecting strange attractors in turbulence. In: Rand DA, Young LS (eds) Dynamical systems and turbulence. Lecture notes in mathematics, Vol 898. Springer-Verlag, New York, NY, p 366–381
Taylor GT, Sullivan CW (2008) Vitamin B12 and cobalt cycling among diatoms and bacteria in Antarctic sea ice microbial communities. Limnol Oceanogr 53:1862–1877
Wallhead PJ, Garçon VC, Casey JR, Lomas MW (2014) Long term variability of phytoplankton carbon biomass in the Sargasso Sea. Global Biogeochem Cycles 28: 825–841
Wheeler PA, Kirchman DL (1986) Utilization of inorganic and organic nitrogen by bacteria in marine systems. Limnol Oceanogr 31:998–1009
Ye H, Beamish RJ, Glaser SM, Grant SC and others (2015) Equation-free mechanistic ecosystem forecasting using empirical dynamic modeling. Proc Natl Acad Sci USA 112:E1569–E1576
Zweifel UL, Norrman B, Hagström Å (1993) Consumption of dissolved organic carbon by marine bacteria and demand for inorganic nutrients. Mar Ecol Prog Ser 101:23–32

Editorial responsibility: Toshi Nagata, Kashiwa, Chiba, Japan

Submitted: August 28, 2017; Accepted: May 21, 2018
Proofs received from author(s): July 11, 2018